

Superdispersible PVP-Coated Fe₃O₄ Nanocrystals Prepared by a “One-Pot” Reaction[†]

Xianyong Lu, Mu Niu, Ruirui Qiao, and Mingyuan Gao*

*Key Laboratory of Colloid, Interface Science and Chemical Thermodynamics, Institute of Chemistry, the Chinese Academy of Sciences, Bei Yi Jie 2, Zhong Guan Cun, Beijing 100190, China**Received: March 22, 2008; Revised Manuscript Received: May 26, 2008*

Poly(*N*-vinyl-2-pyrrolidone) (PVP)-coated Fe₃O₄ nanocrystals were prepared by a “one-pot” synthesis through the pyrolysis of ferric triacetylacetonate (Fe(acac)₃) in *N*-vinyl-2-pyrrolidone (NVP). The polymerization of NVP was followed by measuring the shear viscosity of the reaction mixture. The PVP molecules formed in the reaction mixture was investigated by gel permeation chromatography. As the resultant Fe₃O₄ nanocrystals presented superdispersibility in 10 different types of organic solvents and aqueous solutions with different pH, including 0.01 M phosphate-buffered saline buffer, their hydrodynamic properties in both organic and aqueous systems were investigated by dynamic light-scattering. The results indicated that the PVP-coated Fe₃O₄ nanocrystals can completely be dispersed forming stable colloidal solutions in both organic solvents and water. Fourier transform infrared spectroscopy results suggested that PVP interacted with Fe₃O₄ via its carbonyl groups. Further surface analysis by X-ray photoelectron spectroscopy revealed that there were both coordinating and noncoordinating segments of PVP on the particle surface; the molar ratio between them was of 1:2.6.

Introduction

Magnetic nanoparticles with good dispersibility have found a great number of applications in different fields ranging from pressure seals and rotary shaft seals,¹ to heat dissipating media for high-power loudspeakers,² to recently developed biological assays and biomedical applications such as magnetic drug targeting,³ magnetic resonance imaging contrast agents,⁴ and tumor hypothermia treatment agents.⁵ In principle, two different approaches can be adopted to obtain colloidally stable solutions of the magnetic nanoparticles. The first one relies on the electrostatic interactions between nanoparticles. The second approach relies on the steric stabilization effects introduced by proper surface ligands.⁶ It is quite evident that charge stabilization has limitation in achieving satisfying dispersibility for nanocrystals in a broad range of solvents of various polarities. Therefore, different types of organic modifications have been explored for achieving high-quality nanocrystals with good dispersibility.

In fact, magnetic iron oxide nanocrystals can be prepared by different synthetic routes. But the chemical principles behind the syntheses can generally be classified into two categories. The first group of synthetic routes relies on the hydrolysis of ferric ions and ferrous ions under a proper molar ratio, such as coprecipitation method;⁷ the second group of synthetic routes relies on the pyrolysis of organometallic compounds of iron, such as the thermal decomposition method.⁸ As water and hydroxyl ions have very strong affinity to ferric ions, the organic ligands have to compete against water and hydroxyl ions; therefore, it is difficult to control the surface modification in aqueous systems. In contrast, in the thermal decomposition approach, water is not involved in the reaction, which provides opportunity for organic ligands to approach and eventually bind onto the particle surface via chemical bonds. Therefore,

magnetic nanocrystals with well-defined surface modifications as well as perfect dispersibility are more often seen as the products of thermal decomposition method. For example, magnetic iron oxide nanoparticles stabilized by oleic acid present very good dispersibility in nonpolar solvents.⁸ However, when the surface-bound long alkyl chain molecules are replaced, the dispersibility of the nanocrystals is consequently altered. For example, to replace the stearic acid by poly(ethylene glycol) (PEG)-terminated organic dendrons, the Fe₃O₄ nanocrystals obtained become dispersible in organic solvents such as chloroform, methanol, dimethyl sulfoxide (DMSO), and water.⁹

By thermal decomposition method, we have already established a novel synthetic route for preparing PEG-coated Fe₃O₄ nanocrystals via “one-pot” reaction.^{4a,b} In this synthesis, the PEG-coating was realized during the formation of Fe₃O₄ nanocrystals, and the following sophisticated ligand exchanging process for varying the dispersibility of the magnetic nanocrystals in different solvents was consequently avoided, since PEG chemically bonded on the particle surface enables the resultant nanocrystals be well dissolved in both water and chloroform.

Herein, we report our recent efforts toward this direction. It is well-known that poly(*N*-vinyl-2-pyrrolidone) (PVP) is an amphiphilic polymer that can well be dissolved in a wide range of organic solvents and water.¹⁰ It was expected that PVP molecules derived from the particle surface would help to enhance the dispersibility of the resultant nanocrystals in different types of solvents. Our previous investigations have demonstrated that 2-pyrrolidone can be used as a coordinating solvent in preparing water-soluble Fe₃O₄ nanocrystals.¹¹ Therefore, it is reasonable to use *N*-vinyl-2-pyrrolidone (NVP) as the reaction medium for achieving PVP-coated Fe₃O₄ nanocrystals, based on the fact that ferric triacetylacetonate (Fe(acac)₃), the precursor of Fe₃O₄ nanocrystals, can initiate the polymerization of radical monomers.¹²

[†] Part of the “Janos H. Fendler Memorial Issue”.

* To whom correspondence should be addressed. E-mail: gaomy@iccas.ac.cn. Fax: +86 10 82613214.

Experimental Section

Iron (III) acetylacetonate (Fe(acac)₃) was purchased from Aldrich (14024-18-1, 97%, Aldrich) and used after two recrystallizations. NVP in medical grade was obtained from Jiaozuo Meida Fine Chemical Co., Ltd. It was purified by distillation under reduced pressure in the presence of phenothiazine. All other chemicals of analytical grade were used as received.

1. Synthesis of Fe₃O₄ Nanocrystals. The Fe₃O₄ nanocrystals were synthesized by pyrolyzing Fe(acac)₃ in NVP at 200 °C. Typically, Fe(acac)₃ was first dissolved in NVP at a concentration of 0.04 mol/L. The resultant solution was then purged with argon for 30 min at room temperature to remove oxygen, and subsequently heated to 200 °C. The reaction system was protected by argon throughout the whole reaction process. Different samples were extracted during the reaction at 200 °C. Then an equal portion of ethanol was introduced followed by 5-fold ether as precipitant. Black precipitates were isolated by a permanent magnet. After repeating the above-mentioned procedures for three cycles using ethanol as solvent and ether as precipitant, the magnetic nanocrystals were finally obtained. The samples extracted at 3 and 6 h, denoted as samples A and B, respectively, were chosen for the following investigations.

2. Production Rate of Fe₃O₄ Nanocrystals. The production rate of the reaction was determined by comparing iron content in the final products with that in the initially fed Fe(acac)₃. In detail, a nanocrystal sample was dissolved in hydrochloric acid solution (36.5 wt %). Then excessive hydroxyamine hydrochloride was introduced to completely reduce Fe(III) to Fe(II). The final content of Fe(II) in the solution was determined by phenanthroline method.¹³ The production rates of samples A and B were of 45.3% and 60.2%, respectively.

3. Characterizations. Transmission electron microscope (TEM) images and electron diffraction (ED) patterns were taken on a JEM-100CXII electron microscope at an acceleration voltage of 100 kV. Powder X-ray diffraction (XRD) was performed on a Rigaku D/Max-2500 diffractometer under Cu Kα₁ radiation ($\lambda = 1.54056 \text{ \AA}$). Atomic force microscopy (AFM) was performed with a Digital Instruments Nanoscope IIIa Multimode System (Santa Barbara, CA). The hydrodynamic diameter of the magnetic nanocrystals was determined with a Malvern Zetasizer Nano ZS instrument. The Fourier transform infrared (FTIR) spectroscopy was taken on a Bruker EQUINOX55 FT-IR spectrometer under ambient conditions. The room-temperature shear viscosity of reaction system was followed by TA AR2000 stress-controlled rheometer equipped with two parallel plates of 25 mm in diameter. Gel permeation chromatography (GPC) measurements were performed by a set of Waters 1515 HPLC pumps, a 2414 differential refractometer, and Styragel columns (HT3, HT4, HT5) using dimethylformamide (DMF) as the eluent at 50 °C. X-ray photoelectron spectroscopy data were obtained with an ESCALab220i-XL electron spectrometer from VG Scientific using 300 W Mg Kα radiation. The base pressure was about 3×10^{-9} mbar. Thermogravimetric analysis (TGA) was carried out on a Perkin-Elmer TGA. The samples were analyzed in a temperature range of 20–850 °C with a temperature increasing velocity of 10 °C/min under protection of nitrogen. The magnetic properties of the resultant samples were characterized by a vibrating sample magnetometer (VSM JDM-13, China).

Results

Figure 1 shows the TEM images and ED patterns of particle samples A and B, respectively. Statistical results revealed that the average sizes of sample A and sample B are 4.3 ± 0.8 nm

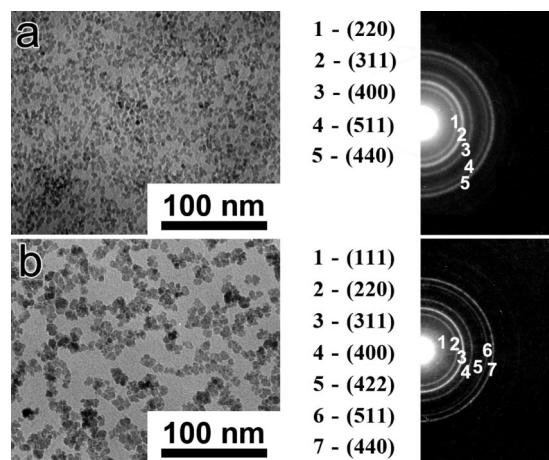


Figure 1. TEM images and ED patterns of sample A (a) and sample B (b).

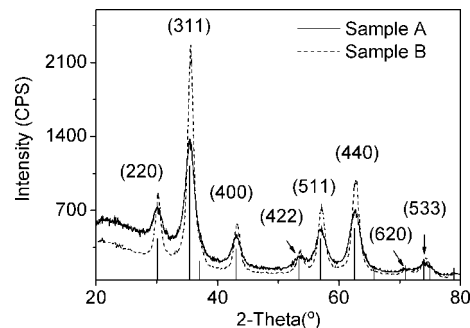


Figure 2. Powder X-ray diffractograms of sample A (solid line) and sample B (dashed line); Bottom: JCPDS card (19-0629) data for magnetite.

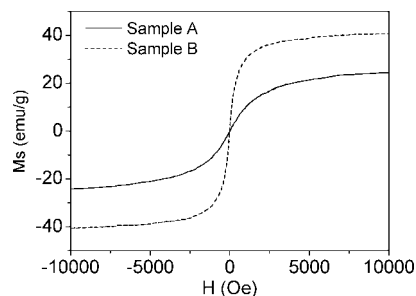


Figure 3. Room-temperature magnetization curves of sample A (solid line) and sample B (dashed line).

and 7.0 ± 1.5 nm, respectively. ED results indicate that both of these two samples are composed of nanostructured materials. Their d -spacing values calculated match well with those from the JCPDS card (No. 19-0629) for magnetite, which were further proven by the XRD measurements shown in Figure 2.

Further TGA measurements revealed that the polymer content in these two samples was 36.2% for sample A and 25.0% for sample B, implying that PVP-coating was successfully realized via the current synthetic route. AFM was used to determine the overall size of the polymer-coated nanoparticles sitting on the surface of mica. Statistical results revealed that the average size of samples A and B were 6.9 ± 2.0 nm and 10.8 ± 1.9 nm, respectively.

The magnetic properties of as-synthesized Fe₃O₄ nanocrystals were measured by vibrating sample magnetometer (VSM). The room-temperature magnetization curves shown in Figure 3 suggest that both samples are superparamagnetic with a saturation magnetization of 24.2 and 40.6 emu/g for samples A and B, respectively.

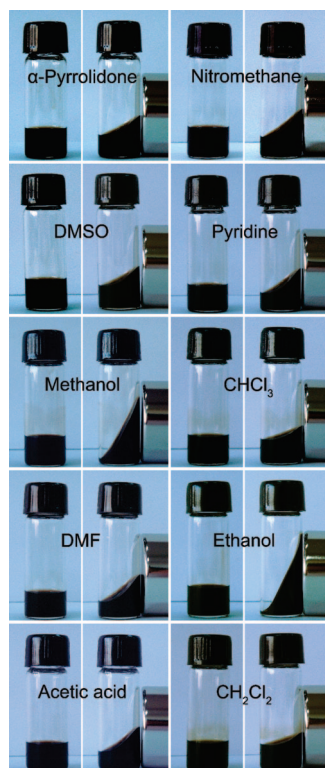


Figure 4. Photographs of sample B dispersed in different types of organic solvents. The photographs were captured in the absence (left) or presence (right) of a permanent magnet.

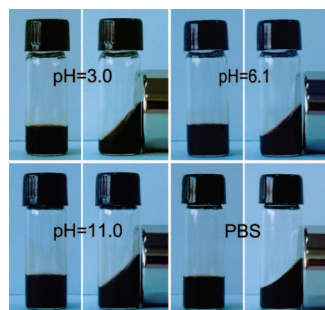


Figure 5. Photographs of sample B dispersed in aqueous solutions of different pH and 0.01 M PBS buffer. The photographs were captured in the absence (left) or presence (right) of a permanent magnet.

The dispersibility of the magnetic nanocrystals was tested by dispersing sample B in different types of solvents at a concentration of 2.3–9.7 mg/mL. Ten different organic solvents, i.e., α -pyrrolidone, DMSO, methanol, DMF, acetic acid, nitromethane, pyridine, CHCl_3 , ethanol, and CH_2Cl_2 , were adopted in addition to water. The polarities of the solvents varied from 3.4 to 10.2 (water). Figure 4 exhibits the photographs of the resultant magnetic fluids, captured in the absence or presence of a permanent magnet. It was found out that the tilt angle of the magnetic fluid surface induced by the external magnetic field strongly depends on the density of the solvent. In addition, the dispersibility of sample B in water of different pH values (3.0, 6.1, 11.0), as well as 0.01 M phosphate-buffered saline (PBS) buffer was also tested, and the photographs of the resultant magnetic fluids are shown in Figure 5.

Discussion

Thermally decomposing organometallic precursors in various nonaqueous media has become a mainstream approach for

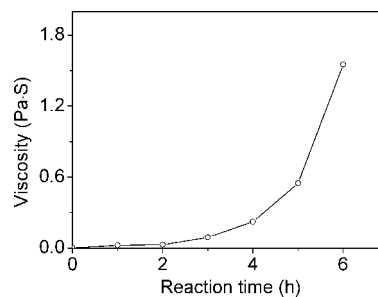


Figure 6. Temporal evolution of the shear viscosity of the reaction solution.

synthesizing high quality nanocrystals. Different from the typical high-boiling-point solvents such as 1-octadecene, phenyl ether, and dioctyl ether, the current synthetic approach adopted strong polar NVP as the reaction media. As NVP is structurally similar to α -pyrrolidone, it was also supposed to be a coordinating solvent.¹¹ In addition, NVP is also a radical monomer that is readily polymerized. Because $\text{Fe}(\text{acac})_3$, as one of most popular precursors used in synthesizing magnetic iron oxide nanocrystals, can also initiate the polymerization of radical monomers, NVP was used as both the coordinating solvent as well as the radical monomer for preparing PVP-coated Fe_3O_4 nanocrystals upon pyrolysis of $\text{Fe}(\text{acac})_3$.

The polymerization of NVP was monitored by measuring the shear viscosity of a 1 mL reaction mixture extracted at a fixed time interval during the reaction. The measurements were performed at 25 °C by a shear rate of 10 s^{-1} . The curve shown in Figure 6 depicts the reaction time-dependent shear viscosity, which increases slowly during the first 3 h, followed by a fast increase until the whole reaction solution became too sticky to be extracted, which strongly suggests that NVP was polymerized and formed PVP during the formation of Fe_3O_4 nanoparticles. The fast increase in the viscosity during the late stage of the reaction is possibly caused by the intermolecular cross-linking of PVP,¹⁴ which is supported by the fact that the magnetic particle samples obtained by a reaction time longer than 6 h presented greatly reduced dispersibility in either organic solvents or water. Therefore, the preparation was generally terminated before 6 h.

The polymerization of NVP was also investigated by FTIR spectroscopy. The FTIR spectra of NVP and samples A and B are provided in the upper frame of Figure 7. The typical vibrational bands of the vinyl group from NVP, located at 1629 cm^{-1} and 983 cm^{-1} , completely disappear in the spectra of both samples A and B,¹⁵ suggesting that NVP has been polymerized. Taking the organic contents, i.e., 36.2% and 25.0% in samples A and B, respectively, into consideration, it can be deduced that PVP formed upon polymerization of NVP is present in the nanocrystal samples. The shift of the vibrational band of the carbonyl group from 1680 cm^{-1} to 1661 cm^{-1} in the nanocrystal samples, however, suggests that PVP is modified on the surface of the Fe_3O_4 nanocrystals via coordination interaction through its carbonyl group.¹⁶ The sharp absorption peak at around 575 cm^{-1} is attributed to lattice absorption of the Fe_3O_4 particles.

The polymerization of NVP was further investigated by measuring the molecular weight of PVP molecules found in liquors containing nanocrystal samples A and B, respectively, using the GPC method. The results are shown in Figure 7. The number-average molecular weight of PVP was determined to be 5.17×10^4 and 4.14×10^4 , respectively, using polystyrene standards as references. The slight decrease in molecular weight of PVP found in liquors containing sample B is probably caused

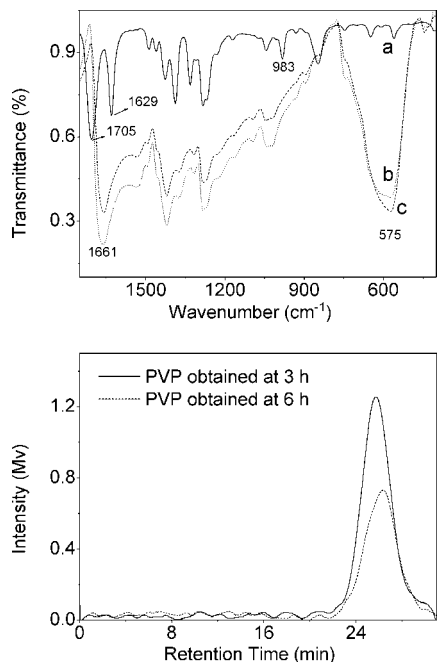


Figure 7. Upper frame: FTIR spectra of NVP (a), sample A (b), and sample B (c). Lower frame: GPC traces of PVP presented in the liquors extracted at 3 h (solid line) and 6 h (dashed line) during the reaction.

by intermolecular cross-linking among higher molecular weight PVP, which eventually leads to nonsoluble gel. In fact, NVP is also a thermal polymerization monomer. Nevertheless, the polydispersity index (PDI) of PVP found in reaction mixtures containing sample A and sample B was calculated to be 1.18 and 1.27, respectively, which somehow suggests that, even if the thermal polymerizing mechanism took effect, it would not be a dominant procedure as the thermal polymerization often gives rise to a much higher PDI.

As the Fe₃O₄ nanocrystals presented very good dispersibility in different types of organic solvents as shown in Figure 4, their hydrodynamic properties were investigated for excluding suspensions of particle aggregations. The hydrodynamic size of sample B in the following solvents, i.e., α -pyrrolidone, DMSO, methanol, DMF, acetic acid, nitromethane, pyridine, CHCl₃, ethanol, and CH₂Cl₂, was determined to be 29.1 nm, 33.7 nm, 28.8 nm, 26.1 nm, 24.8 nm, 22.3 nm, 31.2 nm, 18.8 nm, 25.5 and 38.3 nm, respectively. In general, the hydrodynamic size of the magnetic nanocrystals varies in different type of solvents, but in a very small size regime. This variation is probably caused by the difference in the solubility parameter of the solvents, even though no regular dependency is found. Nevertheless, the hydrodynamic properties of the magnetic nanocrystals strongly support that the magnetic nanocrystals are well dispersed in all the above-mentioned solvents with particles being separated from each other.

In addition to organic solvents, the Fe₃O₄ nanocrystals obtained also present good dispersibility in aqueous solution. The hydrodynamic sizes of sample B were measured in aqueous solutions of different pH values (2.0, 3.0, 5.0, 6.1, 7.4, 9.0, 11.0) by the DLS method, and the results are given in Table 1. In general, the hydrodynamic size of sample B presents very small pH-dependent effects, ranging from 18 to 24 nm. The relatively pH-independent hydrodynamic size suggests that the nanocrystals present very good colloidal stability in a very broad pH range. Moreover, the nanocrystal solutions present a very good long-term stability. In neutral pH range, the colloidal solution remains highly stable for more than 1 year in a refrigerator.

TABLE 1: The Hydrodynamic Size of Sample B in Aqueous Solution with Different pH

pH value	2.0	3.0	5.0	6.1	7.4	9.0	11.0
hydrodynamic size (nm)	20.3	21.9	21.1	18.3	20.7	24.6	22.1
fwhm (nm)	5.8	6.5	6.4	6.1	6.3	6.6	6.3

Since the dispersibility of the nanocrystals in physiological saline is a very important prerequisite for biomedical applications of the magnetic nanocrystals, the dispersibility of sample B was also tested in 0.01 M PBS buffer. The hydrodynamic size was determined to be 20.7 nm, suggesting that the as-prepared Fe₃O₄ nanocrystals can well be dissolved in buffer saline.

The superdispersibility of the Fe₃O₄ nanocrystals is undoubtedly attributed to the surface-bound PVP. Although FTIR spectroscopy results indicate that PVP molecule coordinates with Fe₃O₄ particles via its carbonyl group, more detailed information regarding the surface binding situation remains important to reveal the superdispersibility of the resultant Fe₃O₄ nanocrystals. To fulfill this task, systematic XPS investigations were performed. The survey XPS spectrum of sample B together with the spectra of O 1s and N 1s are shown in Figure 8. All the binding energies are calibrated with reference to C 1s (284.8 eV) of adventitious carbon. The spectra of O 1s and N 1s were fitted by multiple Gaussians with an equal full width at half-

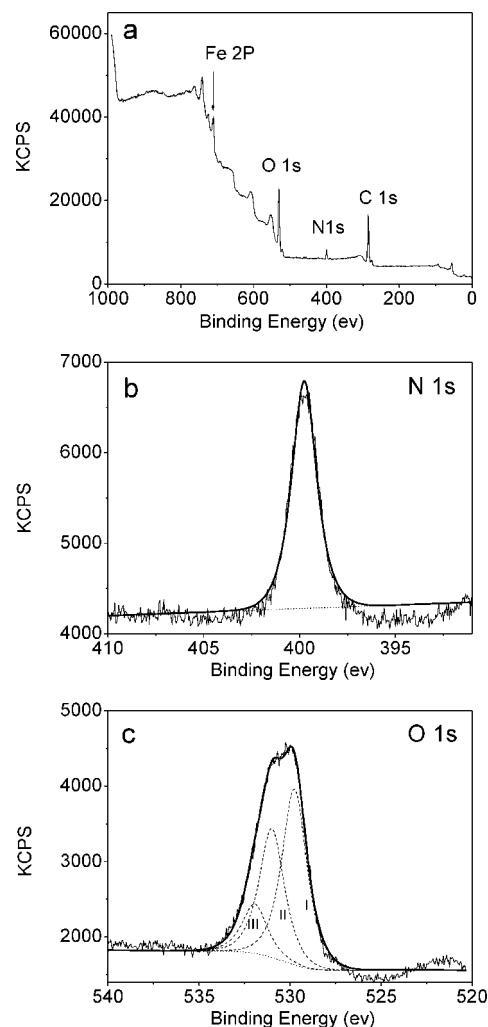


Figure 8. Survey X-ray photoelectron spectrum (a), N 1s (b) and O 1s (c) spectra of sample B. The bold lines shown in frames b and c are the best fits for N 1s and O 1s, respectively.

maximum (fwhm) using a Shirley-type background. The fitting results reveal that the binding energy of N 1s remains unchanged in comparison with that in pure PVP,¹⁷ further supporting that PVP coordinates with Fe₃O₄ nanocrystals via its carbonyl group. The O 1s line was fitted with a convolution of three peaks, i.e., 529.8, 531.0, and 531.9 eV, corresponding to three different O chemical states. According to reference data, the first peak can be assigned to O from magnetite,¹⁸ the second peak (531.0 eV) can be assigned to uncoordinating O in PVP,¹⁷ while the last peak can be attributed to O from PVP coordinating with the Fe₃O₄ nanocrystals.¹⁹ On the basis of this analysis, the ratio between the coordinating and noncoordinating PVP segments is approximately 1:2.6, well interpreting the superdispersibility of the Fe₃O₄ nanocrystals stabilized by PVP since the coordinating PVP segments offer stabilization effects to the Fe₃O₄ nanocrystals and prevent them from uncontrollable growth, while the noncoordinating PVP segments provide the resultant nanocrystals dispersibility in different types of solvents.

Conclusion

In summary, PVP-coated Fe₃O₄ nanocrystals were prepared by a "one-pot" synthesis through the pyrolysis of Fe(acac)₃ in NVP. In this synthetic route, Fe(acac)₃ serves as the precursor of magnetite, and NVP serves as a radical monomer of PVP. Both FTIR and XPS results reveal that the resultant PVP coordinates with Fe₃O₄ nanocrystals via carbonyl groups, as the noncoordinating segment is 2.6 times that of the coordinating segments of PVP. Consequently, the resultant PVP-coated Fe₃O₄ nanocrystals present similar dissolvability to pure PVP and can form stable solutions in a great number of organic solvents as well as water solutions of different pH (including PBS buffer). All these results demonstrate that the current synthetic route is very facile and effective for achieving highly soluble and colloidally stable Fe₃O₄ nanocrystals. Their superdispersibility in both organic and aqueous media may offer potential applications of the superparamagnetic nanocrystals in different fields.

Acknowledgment. The current investigations were financially supported by NSFC projects (20673128, 20640430564) and 863 projects (2006AA02Z479, 2007AA02Z467).

References and Notes

- (1) Black, T.; Raj, K.; Tsuda, S. *J. Magn. Magn. Mater.* **2002**, *252*, 39.
- (2) Odenbach, S. *J. Phys.: Condens. Matter* **2004**, *16*, R1135.
- (3) (a) Lübke, A. S.; Alexiou, C.; Bergemann, C. *J. Surg. Res.* **2001**, *95*, 200. (b) Ganguly, R.; Gained, A. P.; Sen, S.; Puri, I. K. *J. Magn. Magn. Mater.* **2005**, *289*, 331.
- (4) (a) Li, Z.; Wei, L.; Gao, M.; Lei, H. *Adv. Mater.* **2005**, *8*, 1001. (b) Hu, F.; Wei, L.; Zhou, Z.; Ran, Y.; Li, Z.; Gao, M. *Adv. Mater.* **2006**, *18*, 2553. (c) Song, H.-T.; Choi, J.-S.; Huh, Y.-M.; Kim, S.; Jun, Y.-W.; Suh, J.-S.; Cheon, J. *J. Am. Chem. Soc.* **2005**, *127*, 9992.
- (5) (a) Hiergeist, R.; Andrá, W.; Buske, N.; Hergt, R.; Hilger, I.; Richter, U.; Kaiser, W. *J. Magn. Magn. Mater.* **1999**, *201*, 420. (b) Gonzales, M.; Krishnan, K. M. *J. Magn. Magn. Mater.* **2005**, *293*, 265.
- (6) (a) Thomas, K. G.; Ipe, B. I.; Sudeep, P. K. *Pure Appl. Chem.* **2002**, *74*, 1731. (b) Roucoux, A. *Top. Organomet. Chem.* **2005**, *16*, 261.
- (7) (a) Dumazet-Bonnamour, I.; Percec, P. *Colloid Surf., A* **2000**, *173*, 61. (b) Pardoe, H.; Chua-anusorn, W.; Pierre, T. G. S.; Dobson, J. *J. Magn. Magn. Mater.* **2001**, *225*, 41. (c) Wan, S.; Zheng, Y.; Liu, Y.; Yan, H.; Liu, K. *J. Mater. Chem.* **2005**, *15*, 3424.
- (8) (a) Sun, S.; Zeng, H. *J. Am. Chem. Soc.* **2002**, *124*, 8204. (b) Park, J.; An, K.; Hwang, Y.; Park, J. G.; Noh, H. J.; Kim, J. Y.; Park, J. H.; Hwang, N. M.; Hyeon, T. *Nat. Mater.* **2004**, *3*, 891. (c) Jana, N. R.; Chen, Y.; Peng, X. *Chem. Mater.* **2004**, *16*, 3931. (d) Casula, M. F.; Jun, Y.; Zaziski, D. J.; Chan, E. M.; Corrias, A. C.; Alivisatos, A. P. *J. Am. Chem. Soc.* **2006**, *128*, 1675.
- (9) Kim, M.; Chen, Y.; Liu, Y.; Peng, X. *Adv. Mater.* **2005**, *17*, 1429.
- (10) Cui, Y. D.; Yi, G. B.; Liao, L. W. *Synthesis and Applications of Poly(N-vinyl-2-pyrrolidone)*; Science Press: China, 2001.
- (11) (a) Li, Z.; Chen, H.; Bao, H.; Gao, M. *Chem. Mater.* **2004**, *16*, 1391. (b) Li, Z.; Sun, Q.; Gao, M. *Angew. Chem., Int. Ed.* **2005**, *44*, 123.
- (12) Prabha, R.; Nandi, U. S. *J. Polym. Sci., Polym. Lett. Ed.* **1976**, *14*, 19.
- (13) Taras, M. J.; Greenberg, A. E.; Hoak, R. D.; Rand, M. C. *Standard Methods for the Examination of Water and Wastewater*, 13th ed.; American Public Health Association: Washington, DC, 1971.
- (14) (a) Yoshida, M.; Prasad, P. N. *Appl. Opt.* **1996**, *35*, 1500. (b) Zheng, M.-P.; Jin, Y.-P.; Jin, G.-L.; Gu, M.-Y. *J. Mater. Sci. Lett.* **2000**, *19*, 433.
- (15) Doneux, C.; Caudano, R.; Delhalle, J.; Léonard-Stibbe, E.; Charlier, J.; Bureau, C.; Tanguy, J.; Lécayon, G. *Langmuir* **1997**, *13*, 4898.
- (16) Nemanmcha, A.; Rehspringer, J.-L.; Khatmi, D. *J. Phys. Chem. B* **2006**, *110*, 383.
- (17) Beamsom, G.; Briggs, D. *High Resolution XPS of Organic Polymers: The Scienta ESCA300 Database*; John Wiley & Sons: Chichester, U.K., 1992.
- (18) (a) Krasnikov, S. A.; Vinogradov, A. S.; Hallmeier, K. H.; Höhne, R.; Ziese, M.; Esquinazi, P.; Chass, T.; Szargan, R. *Mater. Sci. Eng. B* **2004**, *109*, 207. (b) Zhang, Y.; Sun, C.; Kohler, N.; Zhang, M. *Biomed. Microdevices* **2004**, *6*, 33.
- (19) Lee, H. Y.; Lim, N. H.; Seo, J. A.; Yuk, S. H.; Kwak, B. K.; Khang, G.; Lee, H. B.; Cho, S. H. *J. Biomed. Mater. Res., Part B: Appl. Biomater.* **2006**, *79B*, 142.

JP8025072